Chapter 14
Mössbauer Analysis

Ko Mibu, Masaaki Tanaka and Kohei Hamaya

Abstract As a powerful experimental tool to examine local crystallographic and magnetic environments of Heusler alloy films, Mössbauer spectroscopy is introduced briefly in this section. This method, which is applicable easily when the alloy contains Fe or Sn as a constituent element, can give us unique information on the local degree of structural order, the magnetic stability at the interfaces, and so on.

Mössbauer spectroscopy is an experimental method where local electronic states in solids can be studied through absorption spectra of γ-rays by the constituent nuclei in the solids [1–3]. The energy levels of nuclei are influenced by the surrounding electrons through the hyperfine interactions so that the absorption spectra contain information on local electronic states, including magnetism. The applicability of this experimental method is highly dependent of the sort of nuclei or isotopes and the most easily applicable nuclei in the level of university laboratories are ^{57}Fe (the natural abundance 2.2 %) and ^{119}Sn (the natural abundance 8.6 %). Since some Heusler alloys contain Fe or Sn as an ingredient, Mössbauer spectroscopy can be a powerful tool to elucidate local electronic states of Heusler alloys. Some pioneering works on bulk Heusler alloys are introduced already in a review book on Mössbauer spectroscopy published in 1971 [1] and many papers have been published so far. The number of papers including Mössbauer spectroscopic study on Heusler alloys started increasing again in 2004, boosted by the progress in spintronics, and some of these recent papers have been highly sited up to date [4, 5]. In this section, we focus exclusively on Mössbauer spectroscopic studies about epitaxial Heusler alloy films,

K. Mibu (✉) · M. Tanaka
Graduate School of Engineering, Nagoya Institute of Technology,
Nagoya 466-8555, Japan
e-mail: k_mibu@nitech.ac.jp

M. Tanaka
e-mail: mtanaka@nitech.ac.jp

K. Hamaya
Graduate School of Engineering Science, Osaka University,
Toyonaka 560-8531, Japan
e-mail: hamaya@ee.es.osaka-u.ac.jp

C. Felser and A. Hirohata (eds.), *Heusler Alloys*,
Springer Series in Materials Science 222, DOI 10.1007/978-3-319-21449-8_14

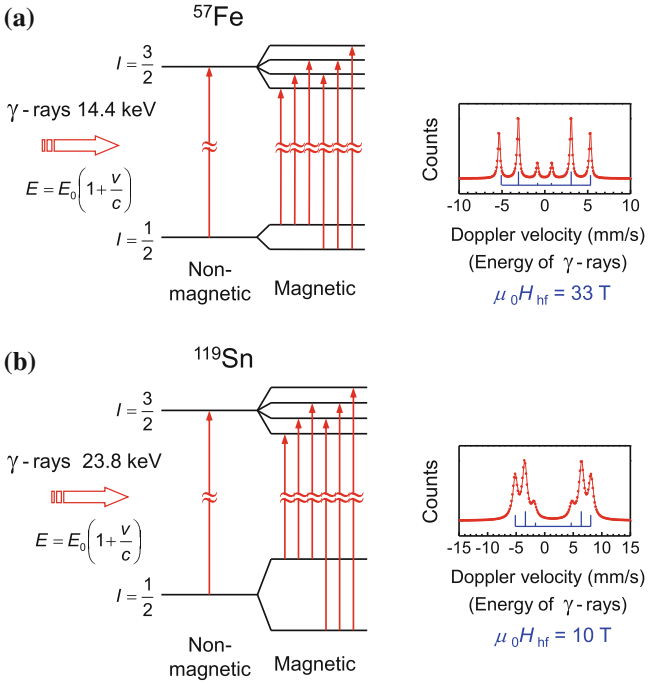

Fig. 14.1 Mössbauer-related energy levers for (**a**) ^{57}Fe and (**b**) ^{119}Sn nuclei in nonmagnetic and magnetic environments. Typical Mössbauer spectra with a magnetically-split six-line pattern are also shown on the *right*

which started appearing in literature around 2007, mainly on the studies performed by our research group.

Figure 14.1 shows typical Mössbauer-related energy levers of ^{57}Fe and ^{119}Sn nuclei and corresponding ^{57}Fe and ^{119}Sn Mössbauer spectra in magnetic environments. Both nuclei have the ground state with the nuclear spin $I = 1/2$ and the first exited state with $I = 3/2$. When the nuclei feel an effective magnetic field, the energy revels are split into 2 and 4 sublevels, respectively. On the occasion of γ-ray absorption, 6 transitions are usually allowed between the sublevels, so that a six-line pattern is observed in the absorption spectra. The effective magnetic field in magnetic materials is called "magnetic hyperfine field" because it originates from the hyperfine interaction between the nuclei and electrons. For usual experiments, a radioisotope is used as the γ-ray source and the energy of the highly monochromatic γ-rays is modulated through the Doppler effect by giving the velocity to the γ-ray source. The abscissa of the spectra is therefore expressed by the Doppler velocity, which is linearly correlated with the energy of the incident γ-rays, instead of being expressed by the units of energy. The center of the gravity of the spectra reflects the charge density of electrons at the nuclear sites and the deviation from the standard position (usually the deviation relative to the center of the spectrum of α-Fe or $CaSnO_3$) is called "isomer shift". The energy levels of the nuclei, hence the absorption spectra, are also

affected by the electric field gradient at the nuclear sites, but this effect is negligibly small in the case of Heusler alloys, where the crystallographic structures basically have cubic symmetry. For epitaxial thin films grown on single crystal substrates, absorption spectra are usually recorded by detecting internal conversion electrons and other secondary electrons, which are resonantly emitted from the sample right after the absorption of γ-rays, in a scattering geometry. This method is called "conversion electron Mössbauer spectroscopy (CEMS)" and the spectra appear as upward peaks as in Fig. 14.1. For magnetic thin films with the magnetic moment in the film plane, as is usual in ferromagnetic Heusler alloy films, the direction of the magnetic hyperfine field is also along the film plane. In such cases the intensity ratio of the six lines becomes 3:4:1:1:4:3, as shown in Fig. 14.1.

In stoichiometric X_2YZ Heusler alloys with an ideal $L2_1$-ordered structure, the atoms of each constituent element occupy a specific crystallographic site, i.e., the 8c site of the $Fm\bar{3}m$ space group for X, the 4b site for Y, the 4a site for Z, so that each element has a single sort of local environments. The Mössbauer spectra for one of the constituent element therefore consist of one six-line pattern when the alloy is magnetically ordered or one single-line pattern when the alloy is nonmagnetic. In off-stoichiometric cases or disordered cases, there appears distribution in the local environments of each constituent element so that the spectra become multiple six-line or single-line patterns or, instead, show line broadening. For such cases, each spectrum component (subspectrum) is usually attributed to a nuclear site which is classified by the sort and number of the atoms at the nearest-neighboring sites. For example, in ferromagnetic Co_2FeZ (Z = Si, Ge, Sn) alloys, each Fe atom is surrounded by 8 nearest-neighboring Co atoms when the Fe is at the proper site (the 4b site) in an ideal $L2_1$ structure, whereas it is surrounded by 4 nearest-neighboring Fe atoms and 4 nearest-neighboring Z atoms when it is at the Co site (the 8c site) due to off-stoichiometry or structural disorder. The Fe nuclei at the latter site are expected to feel smaller magnetic hyperfine field than those at the former site. The effects from the 6 next-nearest-neighboring atoms are usually small in comparison with those from the 8 nearest-neighboring atoms. In this way, Mössbauer analyses can be used to study the local or short-range environments of the constituent atoms in Heusler alloys, as NMR analyses can be [6]. This situation has been well-demonstrated for bulk $L2_1$ Heusler alloys, for example, in [7] and [8]. The first part of this section is devoted to these kinds of analyses on structural order of epitaxial Heusler alloy films. Another effective way to apply Mössbauer spectroscopy to Heusler alloy films is to check the local electronic states, especially magnetism, at the interfaces, which can be highly correlated with the magnetoresistance features of Heusler-alloy-based multilayers or magnetic tunnel junctions. This point is discussed in the latter part of this section.

The validity of the Mössbauer analysis for the study of site occupation is well-demonstrated for "pseudo-Heusler" or "binary Heusler" Fe_3Si alloy films with $D0_3$ structure [9–12]. In this structure, the 8c site and the 4b site in the $Fm\bar{3}m$ space group are occupied by the atoms of the same element, in the case of Fe_3Si, by Fe. Here, each Fe atom at the 8c site has 4 Fe atoms and 4 Si atoms at the nearest-neighboring sites, and that at the 4b site has 8 Fe atoms at the nearest-neighboring sites. It is

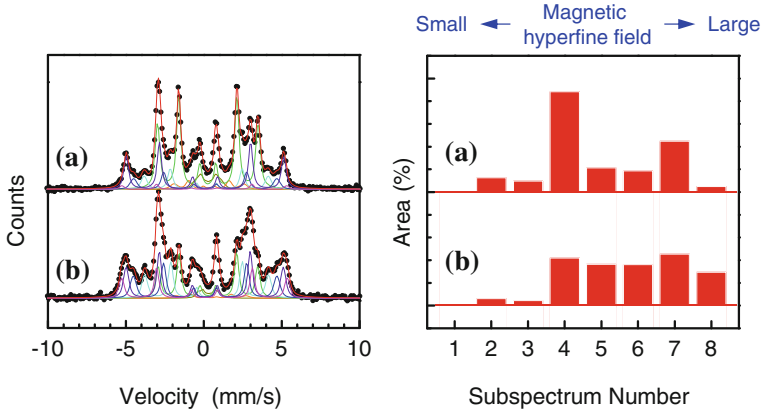

Fig. 14.2 ^{57}Fe Mössbauer spectra of epitaxial (**a**) $Fe_3Si(111)$ (25 nm) and (**b**) $Fe_{3.2}Si_{0.8}(111)$ (30 nm) films on Ge(111) substrates prepared by low-temperature molecular beam epitaxy [10]. Each spectrum is fitted with 7 magnetically-split six-line patterns (7 subspectra), each of which is attributed to the Fe site with a different number of nearest-neighboring Fe and Si atoms. The relative area of each subspectrum is shown on the *right*

known from an experimental study for bulk Fe_3Si [13] that the magnetic hyperfine field for the Fe nuclei at the 8c site (∼20 T) is about 2/3 of that for the Fe atoms at the 4b site (∼31 T). The electron charge density at both sites is also different. Eventually Mössbauer spectrum appears as superposition of two magnetically-split sex-line patterns with different magnetic hyperfine fields and different isomer shifts, with the integrated peak intensity ratio of 2:1. For thin films, where the samples are prepared through non-equilibrium process, it is usually not easy to exclude off-stoichiometry and structural disorder. Figure 14.2 shows the ^{57}Fe Mössbauer spectra of epitaxial $Fe_3Si(111)$ (25 nm) and $Fe_{3.2}Si_{0.8}(111)$ (30 nm) films on Ge(111) substrates prepared by low-temperature molecular beam epitaxy [10]. For the film growth, the Fe source was enriched with the ^{57}Fe isotope up to 20 %, to obtain better S/N ratios in shorter measurement time. The spectra can be fitted with superposition of 7 six-line patters, i.e., 7 magnetic subspectra, as shown in the figure. The intensity ratios of the subspectra are shown on the right, with each subspectrum numbered from 2 to 8 in the order of the magnitude of magnetic hyperfine fields (5.0, 13.9, 20.0, 24.7, 28.5, 31.3, and 32.8 T in the case of $Fe_3Si(111)$). Each subspectrum can be attributed to the Fe site with a different number of nearest-neighboring Fe and Si atoms, according to the analyses on the spectra of bulk samples [13]. The Fe site which has more Fe atoms at the nearest-neighboring sites has a larger magnetic hyperfine field and a smaller (more negative) isomer shift. Subspectra 2, 3, 4, 5, 6, and 7 correspond to the Fe sites in the $D0_3$ phase with the number of nearest-neighboring Fe atoms $0 \sim 2$, 3, 4, 5, 6, $7 \sim 8$, respectively. Subspectrum 8 is from the Fe site in the A2 or bcc phase. A nonmagnetic single-line subspectrum, which is later assigned as Subspectrum 1 for other Heusler alloy systems, is not clearly separable in these spectra. Obviously, for the stoichiometric $Fe_3Si(111)$ film, the Fe site with 4 Fe atoms (Subspectrum 4)

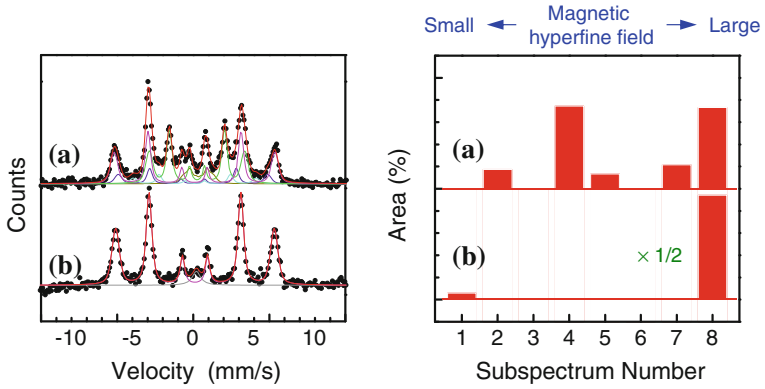

Fig. 14.3 ^{57}Fe Mössbauer spectra of epitaxial (**a**) $Fe_2CoSi(111)$ (25 nm), and (**b**) $Co_2FeSi(111)$ (50 nm) films prepared on Ge(111) substrates by low-temperature molecular beam epitaxy [14, 15]. Each spectrum is fitted with 5 or 2 subspectra. The relative area of each subspectrum is shown on the *right*

and that with 8 Fe atoms (Subspectrum 7) at the nearest neighbors are dominant, suggesting that the epitaxial films basically have a highly ordered $D0_3$ structure. The existence of the component with other Fe coordination numbers indicates that a certain degree of disorder exists in these films, and the degree of disorder is found larger for the off-stoichiometric $Fe_{3.2}Si_{0.8}(111)$ film. With a simple assumption, the local degree of structural order is estimated to be 67 % for the stoichiometric $Fe_3Si(111)$ film grown at 130 °C [10]. This value is sufficiently high for the film grown at such a low temperature. The degree of order tends to increase as the thickness of the films increases, which suggests that the structural disorder gets smaller as the position becomes away from the interface [12]. In this way, it is possible to examine which growth conditions are optimal to grow crystallographically well-ordered Heusler alloy films from Mössbauer spectroscopic measurements. Similar analyses are reported also for epitaxial $Fe_3Si(001)$ films grown on MgO(001) or GaAs(001) substrates [9, 11].

When the Fe atoms in Fe_3Si are replaced by Co atoms to be Fe_2CoSi and Co_2FeSi, the ^{57}Fe Mössbauer spectra change as in Fig. 14.3 [14, 15]. The spectrum of the Fe_2CoSi (111) (25 nm) film on Ge(111) can be fitted with 5 magnetic subspectra as in Fig. 14.3a [14]. Each subspectrum corresponds to the Fe site with a different number of nearest-neighboring Fe atoms. The subspectrum with the largest magnetic hyperfine field of 32.8 T is named as Subspectrum 8, as in the case of Fe_3Si. This subspectrum is from the Fe site with 8 magnetic atoms (Fe or Co) at the nearest-neighboring sites, the crystallographically equivalent component to Subspectrum 7 in Fe_3Si. The magnetic hyperfine field at this Fe site of Fe_2CoSi is enhanced by the existence of Co. Subspectrum 4 with the magnetic hyperfine field of 19.4 T, which can be attributed to the Fe site with 4 magnetic atoms and 4 Si atoms at the nearest neighbors, is also dominant. If the 8c site is occupied by Fe and Co atoms ideally with the ratio of 1:1, the ratio between Subspectrum 4 and 8 should be

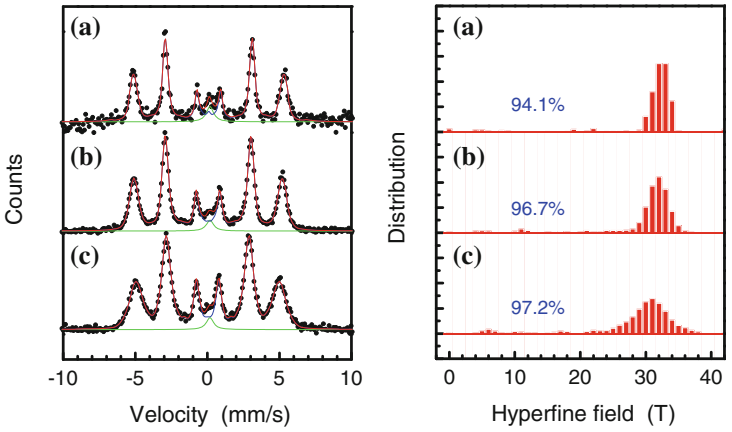

Fig. 14.4 ^{57}Fe Mössbauer spectra of epitaxial (**a**) $CoFe_2Si(111)$ (50 nm) [17], (**b**) $Co_2FeSi_{0.5}Al_{0.5}(111)$ (25 nm) and (**c**) $Co_2FeAl(111)$ (25 nm) films prepared on Si(111) substrates by low-temperature molecular beam epitaxy. Each spectrum is fitted with a distribution of magnetic hyperfine fields with a small amount of nonmagnetic singlet. The distribution is shown on the *right*, with the total area of the magnetic component indicated in percentage

1:1. The observed spectrum and its analysis in Fig. 14.3a are close to this situation, although there also exist other Fe environments. The spectrum of the Co_2FeSi (111) (50 nm) film (made of non-enriched natural Fe) on Ge(111), on the other hand, can be fitted with one magnetic subspectrum with 32.3 T (Subspectrum 8) and one nonmagnetic subspectrum with 0 T (Subspectrum 1), as shown in Fig. 14.3b [15]. The disappearance of Subspectrum 4 shows that the Fe atoms in the 8c site are perfectly repelled by the Co atoms. Therefore, it can be concluded that this film has a highly $L2_1$ or B2 ordered structure without having an A2-type disorder. Note that ^{57}Fe Mössbauer spectra are not so sensitive to the difference between the $L2_1$ and B2 structures because the Fe site has 8 Co atoms at the nearest-neighboring sites in both structures. The effect from the next-nearest-neighboring atoms possibly causes slight peak broadening, which is discussed in the next paragraph. The appearance of Subspectrum 1 means that there is a small amount of nonmagnetic component, probably at the interface region [15]. Note that the effect of interfacial diffusion by annealing is examined for epitaxial $Co_2Cr_{0.6}Fe_{0.4}Al$ films grown on MgO(001) substrates with and without an Fe buffer layer [16].

Figure 14.4 shows the ^{57}Fe Mössbauer spectra of $Co_2FeSi(111)$ (50 nm) (made of non-enriched natural Fe) [17], $Co_2FeSi_{0.5}Al_{0.5}(111)$ (25 nm), and $Co_2FeAl(111)$ (25 nm) films on Si(111) substrates prepared by low-temperature molecular beam epitaxy. The spectra appear as magnetically-split six-line patterns with different line widths. Although each spectrum may be composed of some subspectra, the separation among the subspectra is not so clear, unlike the spectra in Figs. 14.2 and 14.3. Each spectrum is therefore fitted with a distribution of magnetic hyperfine fields. Coexistence of a small amount of nonmagnetic singlet, as observed in the spec-

trum in Fig. 14.3b, is taken into consideration. The obtained distribution of magnetic hyperfine fields is also shown in the figure. The component around 20 T (equivalent position to Subspectrum 4) is negligible, which indicates that the amount of Fe atoms at the 8c site is negligibly small. The distribution becomes wider, hence the parks in the spectrum become broader, as Si atoms are replaced by Al atoms. If the degree of B2 disorder (the disorder between Fe and Z in the 4b and 4a sites) is the same for all the three samples, the local environments of Fe, when considered up to the next-nearest-neighboring atoms, should be the most diverse in the $Co_2FeSi_{0.5}Al_{0.5}$ film. The observed result, however, shows that the Co_2FeAl film has larger peak broadening. This fact implies that the degree of the B2 disorder is larger in the Co_2FeAl film than in the Co_2FeSi film, and that the Co_2FeSi film has a highly $L2_1$ ordered structure. Actually, electron diffraction patterns support the existence of the $L2_1$ ordered phase in the Co_2FeSi film [17].

For the application of magnetic Heusler alloy films to the multilayered giant-magnetoresistance structures or magnetic tunnel junctions, it is important to know whether the magnetic order is maintained at the interfaces on nonmagnetic layers. Mössbauer spectroscopy is a powerful tool to study local crystallographic structure and magnetism at buried interfaces in layered structures (Chap. 5 in [3]). As already shown in this section, the coexistence of a small amount of nonmagnetic phase among the major magnetic phases can be detected as a single line in Mössbauer spectra. In magnetic tunnel junctions with (001)-oriented X_2YZ Heusler alloy layers and a MgO(001) barrier, the tunnel magnetoresistance ratio is yet not satisfactorily large as expected from the half metallicity of Heusler alloys and the ratio decreases largely when the measurement temperature increases from low temperatures to room temperature. To find a key to solve this problem, it is quite informative if the sort of the terminating atoms at the interface (whether X or YZ) and the stability of magnetization at the interface at room temperature are clarified experimentally. Mössbauer analysis can give some information on these points. In our group, X_2YZ Heusler alloy films with the (001) orientation have been prepared on MgO(001) substrates by depositing an atomic layer of X, a half an atomic layer of Z and Y alternately in a controlled manner [18, 19]. By this preparation method, the degree of order may be improved and also it might be possible to control the interfacial atomic species.

Mössbauer spectroscopic experiments were performed for epitaxial Co_2MnSn (001) films, where ^{119}Sn is the Mössbauer isotope, prepared on MgO(001) substrates by the atomically controlled alternate deposition. For the film growth, the Sn source was occasionally enriched with the ^{119}Sn isotope, to 97 % at the maximum. Figure 14.5 shows the ^{119}Sn Mössbauer spectrum for a Co_2MnSn(40.2 nm) film, together with that of a reference bulk Co_2MnSn sample prepared by arc melting. Since the peaks from individual subspectra are not well separated unlike the ^{57}Fe Mössbauer spectra in Figs. 14.2 and 14.3, each spectrum is fitted with a distribution of magnetic hyperfine fields as shown in the figure. (Note that the natural line width is larger for ^{119}Sn Mössbauer spectra than that for ^{57}Fe Mössbauer spectra, as shown in Fig. 14.1.) Although Sn is basically a nonmagnetic element, large magnetic hyperfine fields are induced at the Sn nuclear sites of the ferromagnetic alloys through the Fermi contact interaction between the spin polarized conduction electrons

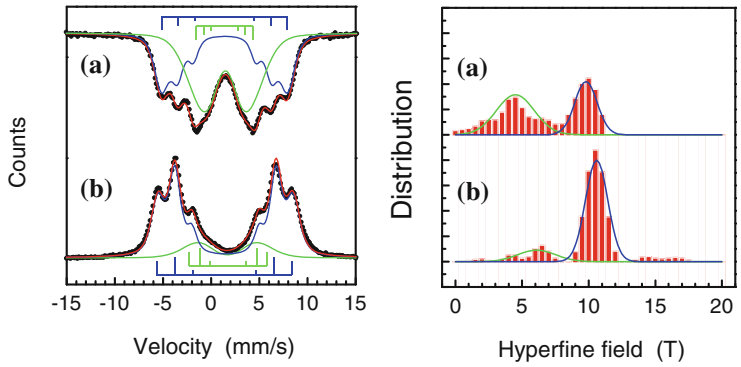

Fig. 14.5 ^{119}Sn Mössbauer spectra and distribution of magnetic hyperfine fields for (**a**) bulk Co_2MnSn Heusler alloy prepared by arc melting (measured with a transmission geometry), and (**b**) an epitaxial $Co_2MnSn(001)$ (40.2 nm) film prepared on a MgO(001) substrate by atomically controlled alternate deposition at 500 °C [19]

and the nuclei. In the arc-melted sample, there are two peaks in the hyperfine-field distribution (at ~4.5 and 10 T), suggesting that there are two Sn environments with different numbers of nearest-neighboring magnetic atoms. Similar spectra are historically reported by other groups [20–22]. Although the origin of the component with the smaller hyperfine field is not clearly assigned, there seems to be Sn atoms at the 8c site. In the film sample made by the atomically controlled alternate deposition, the peak with the smaller magnetic hyperfine field in the distribution histogram becomes much smaller. This means that the Sn atoms in this film sample are with more uniform environments than those in the arc-melted sample. This uniformness in the Sn environments makes it possible to examine the interface magnetism of the Co_2MnSn layers through Mössbauer analyses. Figures 14.6 and 14.7 show the ^{119}Sn Mössbauer spectra and corresponding distribution of magnetic hyperfine fields for $Co_2MnSn(001)$ (2.2 nm)/Ag(001) (3 nm) and $Co_2MnSn(001)$ (2.2 nm)/Cr(001) (3 nm) multilayers. Since the Heusler alloy layers are thinner than those in the sample in Figs. 14.2, 14.3, 14.4, the Mössbauer spectra become more interface-sensitive in these multilayered samples. The deposition order of the Heusler alloy layer is different among the 4 samples, i.e., (a) Co, Mn, Sn, … , Co, (b) Co, Sn, Mn, … , Co, (c) Mn, Sn, Co, … , Mn, Sn, and (d) Sn, Mn, Co, … Sn, Mn. The interfacial atomic layer is "nominally" designed to be Co for the former two samples, and to be MnSn for the latter two samples. The spectra show a couple of experimental facts. First, the spectra look the same independent of the order of atomic deposition and there is no firm evidence that the interface atomic species are controlled as designed. Second, the spectra and the corresponding distribution of magnetic hyperfine fields for the Co_2MnSn/Ag multilayer are similar to those of the thicker $Co_2MnSn(001)$ film in Fig. 14.5b, whereas those for the Co_2MnSn/Cr multilayers are quite different and the reduction of magnetic hyperfine fields is more dominant probably due to the stronger interface effect. The fact that the Co_2MnSn/Ag multilayers have no

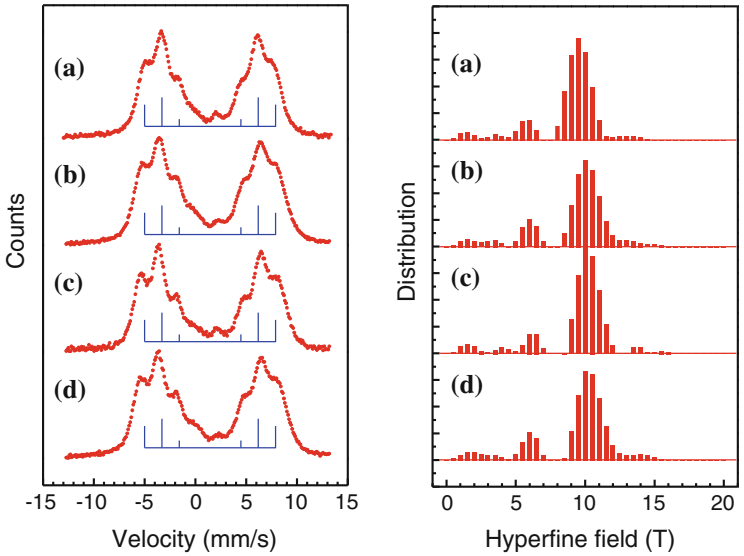

Fig. 14.6 ^{119}Sn Mössbauer spectra and distribution of magnetic hyperfine fields for epitaxial Co_2MnSn(001) (2.2 nm)/Ag(001) (3 nm) multilayers on MgO(001) substrates. **a**, **b**, **c** and **d** are for the samples with the Co_2MnSn layers prepared with different deposition sequences (see the text)

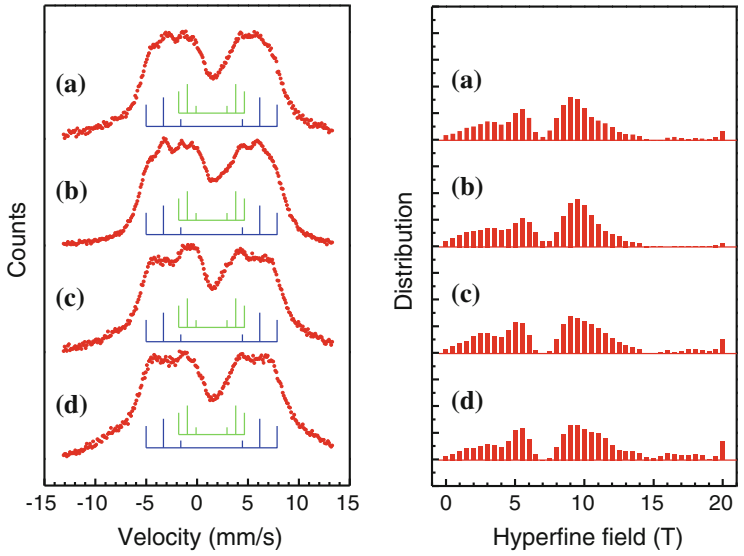

Fig. 14.7 ^{119}Sn Mössbauer spectra and distribution of magnetic hyperfine fields for epitaxial Co_2MnSn(001) (2.2 nm)/Cr(001) (3 nm) multilayers on MgO(001) substrates. **a**, **b**, **c** and **d** are for the samples with the Co_2MnSn layers prepared with different deposition sequences (see the text)

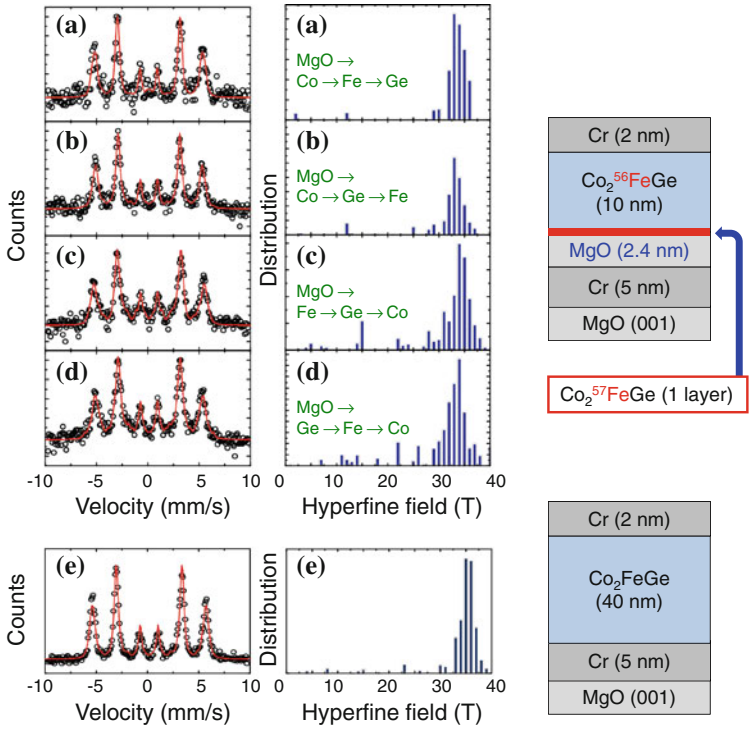

Fig. 14.8 (**a**)–(**d**) ^{57}Fe Mössbauer spectra and distribution of magnetic hyperfine fields for epitaxial $Co_2FeGe(001)$ (10 nm) films on MgO(001) with ^{57}Fe enriched interfaces prepared by atomically controlled alternate deposition [24]. **a**, **b**, **c** and **d** are for the samples prepared with different deposition sequences (see the text). (**e**) ^{57}Fe Mössbauer spectrum and distribution of magnetic hyperfine fields for epitaxial $Co_2FeGe(001)$ (40 nm) film prepared by the same method

reduced magnetic hyperfine field at room temperature suggests that the interfacial magnetization of the Heusler layers, at least in this sample, has no strong reduction at room temperature. Actually there was no strong temperature dependence in the Mössbauer spectra of these multilayers below room temperature.

Similar experiments can be performed for epitaxial $Co_2FeZ(001)$ films [23, 24], where ^{57}Fe is the Mössbauer isotope. Figure 14.8 shows the ^{57}Fe Mössbauer spectra of epitaxial $Co_2FeGe(001)$ films prepared on MgO(001) substrates by alternate deposition of the constituent atoms [24]. Samples with an ^{57}Fe enriched interface, where the Fe at the interfacial atomic layer is composed of the Mössbauer isotope ^{57}Fe, and the rest of the Fe is made of a non-Mössbauer isotope ^{56}Fe, were prepared for more interface-sensitive experiments. The results for the interface-sensitive $Co_2FeGe(001)$ (10 nm) layers are shown in Figs. 14.8a–d. The deposition order in the Heusler alloy layer is different among the 4 samples, i.e., (a) Co, Fe, Ge, … , Co, (b) Co, Ge, Fe, … , Co, (c) Fe, Ge, Co, … , Fe, Ge, and (d) Ge, Fe, Co, … Ge, Fe. Again, there is no clear deposition-order dependence or designed-termination-atom dependence in the

spectra. The spectra and distribution of magnetic hyperfine fields for the films with ^{57}Fe-enriched interfaces are sharp enough, and the value of the magnetic hyperfine field at the peak in distribution is comparable to that of the thicker $Co_2FeGe(001)$ (40 nm) film (non-interface-sensitive sample) in Fig. 14.8e. These results indicate that there is no strong reduction in the magnetization at the Heusler alloy interface at room temperature. On the other hand, the tunneling magnetoresistance effect of the $Co_2FeGe/MgO/Fe$ tunnel junctions, which were prepared with the same procedure, shows strong temperature dependence [24], as reported usually for Heusler-alloy-based magnetic tunnel junctions. There are some suggestions that Heusler alloy films have reduced magnetization at the interface at room temperature and that can be the reason for the reduction of magnetoresistance at room temperature in Heusler-alloy-based magnetoresistance structures [25, 26]. The Mössbauer results imply that the reduction of magnetoresistance at room temperature is not simply due to the temperature-dependent decrease in the interface magnetization [24].

In summary of this section, Mössbauer spectroscopy can be a powerful experimental tool to examine the local environments of Fe or Sn in Heusler alloy films. It can be a tool to judge the local degree of structural order, the magnetic stability at the interfaces, and so on. Recent development of synchrotron-radiation-based Mössbauer spectroscopy would open up new possibility for the researches on electronic states of Heusler alloy films in certain external conditions [27], and also lead to easier accessibility to other Mössbauer elements than Fe and Sn.

References

1. N.N. Greenwood, T.C. Gibb, *Mössbauer Spectroscopy* (Chapman and Hall Ltd., London, 1971)
2. P. Gütlich, E. Bill, A.X. Trautwein, *Mössbauer Spectroscopy and Transition Metal Chemistry* (Springer, Berlin, 2011)
3. Y. Yoshida, G. Langouche (eds.), *Mössbauer Spectroscopy, Tutorial Book* (Springer, Berlin, 2013)
4. S. Wurmehl, G.H. Fecher, H.C. Kandpal, V. Ksenofontov, C. Felser, H.-J. Lin, J. Morais, Phys. Rev. B **72**, 184434 (2005)
5. B. Balke, G.H. Fecher, H.C. Kandpal, C. Felser, K. Kobayashi, E. Ikenaga, J.-J. Kim, S. Ueda, Phys. Rev. B **74**, 104405 (2006)
6. K. Inomata, M. Wojcik, E. Jedryka, N. Ikeda, N. Tezuka, Phys. Rev. B **77**, 214425 (2008)
7. V. Jung, B. Balke, G.H. Fecher, C. Felser, Appl. Phys. Lett. **93**, 042507 (2008)
8. V. Ksenofontov, M. Wójcik, S. Wurmehl, H. Schneider, B. Balke, G. Jakob, C. Felser, J. Appl. Phys. **107**, 09B106 (2010)
9. B. Krumme, C. Weis, H.C. Herper, F. Stromberg, C. Antoniak, A. Warland, E. Schuster, P. Srivastava, M. Walterfang, K. Fauth, J. Minár, H. Ebert, P. Entel, W. Keune, H. Wende, Phys. Rev. B **80**, 144403 (2009)
10. K. Hamaya, T. Murakami, S. Yamada, K. Mibu, M. Miyao, Phys. Rev. B **83**, 144411 (2011)
11. S.I. Makarov, B. Krumme, F. Stromberg, C. Weis, W. Keune, H. Wende, Appl. Phys. Lett. **99**, 141910 (2011)
12. S. Yamada, J. Sagar, S. Honda, L. Lari, G. Takemoto, H. Itoh, A. Hirohata, K. Mibu, M. Miyao, K. Hamaya, Phys. Rev. B **86**, 174406 (2012)
13. M.B. Stearns, Phys. Rev. **129**, 1136 (1963)

14. K. Tanikawa, S. Oki, S. Yamada, K. Mibu, M. Miyao, K. Hamaya, Phys. Rev. B **88**, 014402 (2013)
15. K. Kasahara, K. Yamamoto, S. Yamada, T. Murakami, K. Hamaya, K. Mibu, M. Miyao, J. Appl. Phys. **107**, 09B105 (2010)
16. V. Ksenofontov, C. Herbort, M. Jourdan, C. Felser, Appl. Phys. Lett. **92**, 262501 (2008)
17. S. Yamada, K. Hamaya, K. Yamamoto, T. Murakami, K. Mibu, M. Miyao, Appl. Phys. Lett. **96**, 082511 (2010)
18. W. Zhang, N. Jiko, T. Okuno, K. Mibu, K. Yoshimura, J. Magn. Magn. Mater. **309**, 132 (2007)
19. K. Mibu, D. Gondo, T. Hori, Y. Ishikawa, M.A. Tanaka, J. Phys.: Conf. Ser. **217**, 012094 (2010)
20. J.M. Williams, J. Phys. C **1**, 473 (1968)
21. R.A. Dunlap, R.H. March, G. Stroink, Can. J. Phys. **59**, 1577 (1981)
22. A.G. Gavriliuk, G.N. Stepanov, S.M. Irkaev, J. Appl. Phys. **77**, 2648 (1995)
23. M.A. Tanaka, Y. Ishikawa, Y. Wada, S. Hori, A. Murata, S. Horii, Y. Yamanishi, K. Mibu, K. Kondou, T. Ono, S. Kasai, J. Appl. Phys. **111**, 053902 (2012)
24. M.A. Tanaka, D. Maezaki, T. Ishii, A. Okubo, R. Hiramatsu, T. Ono, K. Mibu, J. Appl. Phys. **116**, 163902 (2014)
25. T. Saito, T. Katayama, T. Ishikawa, M. Yamamoto, D. Asakura, T. Koide, Y. Miura, M. Shirai, Phys. Rev. B **81**, 144417 (2010)
26. Y. Miura, K. Abe, M. Shirai, Phys. Rev. B **83**, 214411 (2011)
27. K. Mibu, M. Seto, T. Mitsui, Y. Yoda, R. Masuda, S. Kitao, Y. Kobayashi, E. Suharyadi, M.A. Tanaka, M. Tsunoda, H. Yanagihara, E. Kita, Hyp. Int. **217**, 127 (2013)